Expression and Knockdown of Cellular Prion Protein (PrPc) in Differentiating Mouse Embryonic Stem Cells

Oscar A. Peralta[a,1], **William R. Huckle**[b], and **Willard H. Eyestone**[a,*]

[a]Department of Large Animal Clinical Sciences, Virginia-Maryland Regional College of Veterinary Medicine, Virginia Polytechnic Institute and State University, Blacksburg, Virginia, USA

[b]Department of Biomedical Sciences and Pathobiology, Virginia-Maryland Regional College of Veterinary Medicine, Virginia Polytechnic Institute and State University, Blacksburg, Virginia, USA

Abstract

The mammalian cellular prion protein (PrP^C) is a highly conserved glycoprotein that may undergo conversion into a conformationally altered isoform (scrapie prion protein or PrP^{Sc}), widely believed to be the pathogenic agent of transmissible spongiform encephalopathies (TSEs). Although much is known about pathogenic PrP conversion and its role in TSEs, the normal function of PrP^C is poorly understood. Given the abundant expression of PrP^C in the developing mammalian CNS and the spatial association with differentiated stages of neurogenesis, recently it has been proposed that PrP^C participates in neural cell differentiation. In the present study, we investigated the role of PrP^C in neural development during early embryogenesis. In bovine fetuses, PrP^C was differentially expressed in the neuroepithelium, showing higher levels at the intermediate and marginal layers where more differentiated states of neurogenesis were located. We utilized differentiating mouse embryonic stem (ES) cells to test whether PrP^C contributed to the process of neural differentiation during early embryogenesis. PrP^C showed increasing levels of expression starting on Day 9 until Day 18 of ES cell differentiation. PrP^C expression was negatively correlated with pluripotency marker Oct-4 confirming that ES cells had indeed differentiated. Induction of ES cells in the presence of retinoic acid (RA) resulted in up-regulation of PrP^C at Day 20 and nestin at Day 12. PrP^C expression was knocked down in PrP-targeted siRNA ES cells between Days 12 and 20. PrP^C knockdown in ES cells resulted in nestin reduction at Days 16 and 20. Analysis in early bovine fetuses suggests the participation of PrP^C in neural cell differentiation during early embryogenesis. The positive association between PrP^C and nestin expression provide evidence for the contribution of PrP^C to ES cell differentiation into neural progenitor cells.

Keywords

Cellular prion protein (PrP^C); neurogenesis; bovine embryogenesis; mouse embryonic stem cells (ESC); nestin; MAP-2

[*]Correspondence to: Willard H. Eyestone, Department of Large Animal Clinical Sciences, Virginia-Maryland Regional College of Veterinary Medicine, Duckpond Drive, Phase II, Blacksburg, Virginia 24061-0442, Phone: 1-540-231-4834, Fax: 1-540-231-1676, weyest@vt.edu.
[1]Present address: Institute of Animal Sciences, Faculty of Veterinary Medicine, Universidad Austral de Chile, Edificio Federico Saelzer, 4to piso, Campus Isla Teja, Valdivia, Chile, Phone: 56-63-293062, Fax: 56-63-221528, oscarperalta@uach.cl

INTRODUCTION

The mammalian cellular prion protein (PrP^C) is a highly conserved glycoprotein localized in membrane lipid rafts and anchored to the cell surface by glycophosphatidylinositol (GPI) [1]. It is present in many cell types, and is particularly abundant in neurons [2]. Under certain conditions PrP^C may undergo conversion into a conformationally-altered isoform (scrapie prion protein or PrP^{Sc}) widely believed to be the pathogenic agent in prion diseases or transmissible spongiform encephalopathies (TSEs) [3,4]. Although much is known about the effect of PrP^{Sc} in prion disease, the normal function of PrP^C is poorly understood. PrP^C binds copper ions, can function as a Cu/Zn superoxide dismutase and has been shown to protect cells against oxidative stress [5]. Alternatively, PrP^C may act as an antiapoptotic agent by blocking some of the internal or environmental factors that initiate apoptosis [6,7]. Despite these putative roles, mice null for PrP^C display no consistent phenotype apart from complete resistance to TSE infection [8,9].

Recently, several authors have proposed that PrP^C participates in transmembrane signaling processes associated with hematopoietic stem cell replication and neuronal differentiation [10,11,12]. Abundant expression of PrP^C has been detected during mouse embryogenesis in association with the developing nervous system [13,14,15]. In the developing mouse brain, undifferentiated neural progenitor cells in the mitotically active ventricular zone do not express PrP^C. In contrast, post-mitotic neurons express high levels of PrP^C after their last mitosis in the neuroepithelium as migrate towards the marginal layers and differentiate [12,15]. Thus, PrP^C may be expressed exclusively in differentiated neurons. Studies in vitro have showed that expression of PrP^C is positively correlated with differentiation of multipotent neural precursors into mature neurons [12]. In addition, treatment of embryonic hippocampal neurons with recombinant PrP^C enhances neurite outgrowth and survival [16].

Given the abundant expression of PrP^C in the developing mammalian CNS and the spatial association with differentiated stages of neurogenesis in the neuroepithelium, we investigated the role of PrP^C in neural development during early bovine embryogenesis (gestation Days 27 and 39; total gestation interval=283 days). The spatial localization of PrP^C in the nervous system of early bovine fetuses was first analyzed. We examined whether PrP^C shared a common location with nestin, a marker of neuronal progenitor cells and MAP-2, a mature neuron marker. PrP^C was differentially expressed in the neuroepithelium, showing higher levels at the intermediate and marginal layers which are occupied by more differentiated neuronal cells. Expression of PrP^C in the nervous system at these early developmental stages suggested that PrP^C might play a role in nervous system development. However, PrP^C levels do not lend themselves to convenient experimental manipulation in the bovine system. Therefore, we chose to examine the effect of siRNA-mediated knockdown of PrP^C in differentiating mouse embryonic stem (ES) cells. We found evidence for a significant contribution of PrP^C in the process of neural cell differentiation.

MATERIAL AND METHODS

Bovine fetuses

Intact early gestation bovine fetuses were obtained from six clinically healthy cows at a local abattoir. Reproductive tracts were obtained at slaughter and gently palpated for the presence of a four-to six-week old fetus (bovine gestation interval=283 days, or about 40 weeks). Though detailed descriptions of early bovine nervous system development have not been made, neural tube closure occurs on Day 22 and the formation of sulci and gyri commences around Day 60 [17]. Thus, fetuses of four-to-six week's gestational age clearly represent early stages of neural development. After extraction from the uterus and placental

membranes, crown-rump length of each fetus was measured in order to estimate fetal age as described in [17]. Fetuses were then fixed in 10% formalin.

Immunohistochemistry

Formalin-fixed fetuses were embedded in paraffin and sectioned at 5–7 µm using a microtome (Historange, LKB Bromma, Sweden). Tissue sections were mounted on adhesive coated slides (Newcomer supply; Middleton, Wisconsin) and incubated overnight at 37°C. Mounted tissues were deparaffinized in xylene and rehydrated in serial alcohol solutions. Slides were subjected to an unmasking protocol by autoclaving at 120°C for 5 min in an unmasking solution (Vector Laboratories, Burlingame, CA, USA). Endogenous peroxidase was blocked by incubation in 3% hydrogen peroxidase diluted in 0.1 M PBS for 30 min. Slides were then rinsed two times in PBS and blocked in 2.5% horse serum for 15 min. Tissues were probed for PrP^C by incubating overnight at RT with 1° antibody (SAF-32, Cayman Chemical Company, Ann Arbor, MI) diluted 1:400 in 1.5 % equine serum (Vector Labs.). Serial slides were probed similarly for nestin using a mouse monoclonal antibody (1:200; 2Q178, Santa Cruz Biotechnology, Santa Cruz Biotech, CA) and for MAP-2 using a mouse monoclonal (1:200; MT-01, Santa Cruz Biotech). After two washes in PBS, bound 1° antibody were detected using pan-specific 2° antibody conjugated to horseradish-peroxidase (Vector Labs.) by incubating for 10 min at RT. Immune complexes were visualized using 3, 3'-diaminobenzidine (DAB) substrate for 5 min or until the signal became visible. Probed sections were then counterstained with hematoxilyn and dehydrated in serial alcohol solutions. Sections were mounted with permount (Fisher Scientific, Hampton, NH) under coverslips. Bovine obex tissue was prepared and probed in parallel to serve as a positive control for PrP^C. The following procedural controls were performed on neighboring sections: 1) replacement of the 1° antibody with non-immune serum, 2) replacement of the 2° antibody with non-immune serum, and 3) omission of both 1° and 2° antibodies, followed by incubation in DAB alone. Digital photos of tissue sections were obtained using bright microscopy (Olympus Vanox-T, Tokyo, Japan).

ES cell culture

Mouse ES cells (D3) and STO feeder cells (SNL) were obtained from ATCC (Manassas, VA, USA) and cultured according to [18]. STO cells were seeded onto 0.1% gelatin-coated 100 mm diameter tissue culture dishes and cultured in DMEM supplemented with 10% fetal bovine serum (FBS) and 50 µg/ml gentamicin. When 80% confluent, STO cells were mitotically-inactivated in 10 µl/ml mitomycin C for 1 h (Sigma Aldrich, St. Louis, MO). Approximately 1×10^6 ES cells were then seeded on feeders in DMEM supplemented with 1% non-essential aminoacids, 10^{-4} M β-mercaptoethanol, 1000 units/ml leukemia inhibitory factor (LIF; Millipore, MA), 15% ES cell-qualified FBS (Hyclone, Logan, UT) and 50 µg/ml gentamicin. Under these conditions, undifferentiated ES cells form typical compacted colonies attached to monolayer of STO cells. Medium was changed every other day and ES cells were detached using 0.25% trypsin and 1 mM EDTA in 0.1% PBS (trypsin/EDTA) and passaged 1:4 onto STO feeders every 3-days.

To initiate differentiation, ES cell were gently harvested when 80% confluent using trypsin/EDTA. Relatively intact ES cell colonies were resuspended in 10 ml ES cell medium in a conical tube separated from STO cells by gravity sedimentation for 10 min. The denser ES cell colonies formed a soft pellet, while most of the STO cells remained in suspension. After discarding the supernatant, the pellet was resuspended in ES cell medium and further separation of ES cells and STO cells was achieved by repeated differential plating after which most STO cells attached to the dish. At this point, the unattached ES cell colonies were reduced in trypsin/EDTA to a monocellular suspension by trituration. To initiate differentiation feeder-depleted ES cells were centrifuged at 200 g for 10 min and

resuspended in differentiation medium (ES cell medium without LIF), seeded into non-adherent plastic bacteriological petri dishes and placed in the incubator. Under these conditions, ES cells aggregated within a few hours and formed embryoid body (EBs). After four days, EBs were disaggregated by trituration in trypsin/EDTA, resuspended in differentiation medium and seeded into plastic tissue culture dishes and cultured for an additional 17 days. Samples were obtained at three-day intervals for 21 days and analyzed for PrP^C and Oct-4 expression by western blot; PrP^C expression was also analyzed by real-time quantitative PCR.

To study the effect of retinoic acid (RA) on ES cell differentiation, ES cells were cultured according to the 4−/4+ protocol reported by [19]. Briefly, ES cells were allowed to form EBs as above for 4 days without RA. At that point, EBs were transferred to fresh differentiation medium supplemented with 5×10^{-7} M of RA. After four days, about 100 EBs were transferred to each of six 35-mm tissue culture dishes in differentiation medium without RA. ES cells were sampled at four-day intervals during the 20-day experimental period and analyzed for expression of PrP^C, Oct-4 and nestin by western blot.

siRNA expression vector

A candidate siRNA target sequence in the murine Prnp coding region was identified using siRNA design software (OligoEngine). A DNA insert designed to encode a shRNA was synthesized by Oligoengine and ligated into the pSUPER.neo vector [20]. A control vector was also made using a scrambled version of the shRNA sequence. Target siRNA and scramble sequences were at follows: AACCAGAACAACUUCGUGC and GGGUAUGGAGAGACACGCA. Positive bacterial clones were identified by PCR across the insertion site and confirmed by DNA sequencing. Clones harboring plasmids with the desired sequences were expanded in 100 ml liquid culture, and plasmids were purified using Qiagen Maxi-prep reagents in preparation for transfection of ES cells (Huckle and Eyestone, unpublished).

Linearized pSUPER.neo (4 µg/ml) was transfected into undifferentiated ES cells using Lipofectamine Plus (Invitrogen). After 24 hours, 800 µl/ml G418 was added to select for neomycin-resistant (neoR) cells over the next 7 days. Clonal lines were established by culturing neoR cells at limiting dilution on mitotically-inactivated STO in 96-well plates. Colonies were expanded to obtain sufficient quantities for PrP^C mRNA and protein analysis (confluent, 60 mm dishes) and cryopreservation (100 mm dishes).

Western blot

ES cells were washed with PBS and homogenized in cold lysis buffer (10 mM Tris, pH 7.4, 150 mM NaCl, 1% Triton-X-100, 1% deoxycholate, 0.1% SDS). Homogenates were centrifuged at 13,500 rpm for 5 min and the supernatants transferred into a new tube. Total protein concentrations were determined using a bicinchoninic acid (BCA) kit (Pierce; Rockford, IL) according to the manufacturing's instructions. Proteins were denatured by mixing the samples 1:1 (v/v) with Laemmli buffer (BioRad Laboratories, Hercules, CA, USA) and heating to 98°C for 5 min. Aliquots containing 20 µg of total protein were loaded in each lane and separated by SDS-PAGE in 12% gels (BioRad) at 125 V. Proteins were then transferred onto PDVF membranes by electroblotting at 100 V for 1h. After blocking for 1 h in blocking buffer (LI-COR Corporation, Lincoln, NE, USA) membranes were probed for PrP^C with a monoclonal antibody SAF-32 (Cayman Chemical, Ann Arbor, MI) diluted 1:400 for 1 h at RT. Additional membranes blotted with protein from the same samples were processed identically with antibodies to nestin (1:200; 2Q178), MAP-2 (1:200; MT-01), Oct-4 (1:500; H-134) (All from Santa Cruz Biotechnology, Santa Cruz, CA). All membranes were co-probed for β-actin using a monoclonal antibody (1:1000;

Santa Cruz Biotechnology). Primary antibodies were diluted in 0.1% Tween-20 in blocking buffer (LI-COR). After four 5 min washes in 0.1% Tween-20 in PBS, membranes were incubated in the appropriate anti-mouse or anti-rabbit IRDye-conjugated secondary antibody (LI-COR) diluted 1:5000 in 0.1% Tween-20 in blocking buffer for 30 min. Immunoreactive band intensities of PrP^C and β-actin were detected and quantified as integrated intensity values using an Odyssey infrared imaging system (LI-COR Corporation). Relative expression of PrP^C was normalized to β-actin expression and standardized to the lowest expression value on Day 0.

RNA Extraction and cDNA synthesis

Approximately 3×10^5 ES cells were collected and immediately fixed in RLT buffer (Qiagen, Incorporated, Valencia, CA). Total RNA was extracted using RNeasy Mini kit (Qiagen Incorporated) according to the manufacturing's instructions. The concentration and purity of the RNA in each sample were determined using Ribogreen RNA quantification kit (Molecular Probes, Eugene, OR). Total RNA was eluted in 30–50 µl of RNase free water. Samples were subjected to RT-PCR using an iScript cDNA synthesis kit (Bio-Rad). The reaction protocol consisted of incubation for 5 min at 25°C, 30 min at 42°C, 5 min at 85°C and hold at 4°C using a DNA engine PCR thermocycler (Bio-Rad).

Quantitative-PCR

Real-time PCR primers and TaqMan probes were designed using PrimerExpress software (Applied Biosystems Incorporated, Foster City, CA) to amplify a segment of cDNA spanning the exon 2-exon 3 junction in the mouse Prnp sequence. Equivalence of amplification efficiencies among all primer-probe sets was confirmed using serial 5-fold dilutions of mouse or bovine brain cDNA (Huckle and Eyestone, unpublished). TaqMan probe sequence (AGCAGACTATCAGTCATCATGGCGAACCTTG) specific for the target was designed to contain a fluorescent 5' reporter dye (FAM) and 3' quencher dye (TAMRA). Sequence of forward and reverse mouse Prnp primers were as follows: AGCATTCTGCCTTCCTAGTGCTA and GAGGGCCAGCAGCCAGTAG. Each RT-PCR reaction (25 µl) contained the following: 2X Master Mix without uracil-N-glycosidase (12.5 µl), 40X Multiscribe and RNase Inhibitor Mix (0.63 µl), target forward primer (60 nM), target reverse primer (60 nM), fluorescent-labeled target probe (4 nM) designed for the RNA sequence isolated form bovine and a total RNA (40 ng). The PCR amplification was carried out in the 7300 Real Time PCR System (Applied Biosystems Incorporated). Thermal cycling conditions were 48°C for 30 min and 95°C for 10 min, followed by 40 repetitive cycles at 95°C for 15 sec and 60°C for 1 min. As a normalization control for RNA loading, parallel reactions in the same multiwell plate were performed using TaqMan Ribosomal RNA as a target (18s control kit, Applied Biosystems). Quantification of gene amplification was made following RT-PCR by determining the threshold cycle (C_T) number for FAM fluorescence within the geometric region of the semilog plot generated during PCR. Within this region of the amplification curve, each difference of one cycle is equivalent to a doubling of the amplified product of the PCR. The relative quantification of the target gene expression across treatment was evaluated using the comparative $\Delta\Delta C_T$ method. The C_T value was determined by subtracting the ribosomal C_T value from the target C_T value of the sample. Calculation of $\Delta\Delta C_T$ involved using Prnp expression on day 0 (sample with the highest CT value or lowest target expression) as an arbitrary constant to subtract from all other C_T sample values. Relative PrP^C mRNA expression was calculated as fold changes in relation to Day 0 sample and expressed as $2^{-\Delta\Delta CT}$ value.

Immunofluorescence

Undifferentiated and differentiated ES cells (cultured 20 days under differentiating conditions as described above) were cultured in 35-mm dishes, fixed in a mixture of

methanol and acetone (1:1) at −20°C for 5 min and stored at 4°C under PBS. Cells were then washed twice in PBS twice and blocked in blocking buffer (LI-COR, blocking buffer, 0.1% Tween-20 in PBS, 1:1) for 30 min at RT. Cells were probed for PrP^C with SAF-32 antibody (1:400; Cayman Chemical) and rabbit anti-nestin (1:200; 2Q178, Santa Cruz Biotechnology) diluted in blocking buffer. After three washes with PBST (PBS, 0.1% Tween-20), cells were incubated with goat anti-rabbit IgG conjugated to Alexa Fluor 488 or goat anti-mouse IgG labeled with Alexa Fluor 594 (both diluted 1:400 in blocking buffer). Then cells were again washed three times in PBST and mounted under coverslips in a solution containing 4', 6-diamidino-2-phenylindole (DAPI; Vector Laboratories). Samples were examined under epifluorescence and the results captured by digital photomicroscopy (Olympus, Tokyo, Japan).

Data Analysis

Cell lysates for each of the three replicates were run in three independent gels and quantified separately. Values of expression of PrP^C were transferred to a spreadsheet and then analyzed using SAS software (version 9.3.1, SAS Institute Inc., Cary, NC). Data was normalized to logarithmic scale in base 10 for normality and mean values for each replicate were compared by one-way ANOVA. PrP^C, Oct-4 and nestin expression values for each day of culture were compared to the sample value on Day 0 using Dunnet's t-test. Significant differences ($P < 0.05$) between days of culture were analyzed using Duncan's multiple comparison test. Differences between treatments for each individual day were compared using student T-test. PrP^C and Oct-4 values for the 21-day period were compared using correlation coefficients.

RESULTS

PrP^C is expressed in the developing bovine nervous system

Immunodetection of PrP^C in bovine fetuses at both Days 27 and 39 of development showed intense expression in the CNS and peripheral nerves (Figs. 1A–D and 2A–D). In the brain and spinal cord, PrP^C was expressed mainly in the intermediate and marginal layers of the neuroepithelium. This region is occupied primarily by axons and dendrites of cortical neurons and neuroglia (Figs. 1E, I and 2E, I). In contrast, PrP^C was not detected in the periventricular zone, a region that contains undifferentiated, mitotically-active neural progenitor cells (Figs. 1E and 2 E). PrP^C immunoreactivity was detected in dorsal root ganglia at Days 27 and 39 (Figs. 1M and 2A) and the peripheral nerves associated with the developing intestine at Day 39 of development (Fig. 2M). Nestin, a marker within the nervous system for proliferating neural progenitor cells [21] was abundantly expressed in tissues of both central (CNS) and peripheral nervous (PNS) systems at Day 27 (Fig. 1B). Within the CNS, nestin expression extended across the neuroepithelium with the most intense staining in the periventricular area indicating presence of proliferating neural progenitor cells (Fig. 1F,J). Nestin was also detected in dorsal root ganglia (Fig. 1N). The overall distribution of nestin expression at Day 39 was similar to Day 27 (Fig. 2B); however at Day 39, nestin was mainly located in the intermediate and marginal layers of the neuroepithelium and in peripheral nerves (Fig. 2F,J,N). Similar to previous reports [22,23], nestin was also detected in non-neural tissues including liver, heart and mesonephros (Figs. 1B and 2B). MAP-2, a marker for mature post-mitotic neurons, was mainly located on Day 27 in the intermediate neuroepithelial region of the CNS (Fig. 1G,K) and in dorsal root ganglia (Fig. 1O). On Day 39, MAP-2 was present in the intermediate region but was absent from the marginal layer (Fig. 2G,K). MAP-2 expression was not detected in peripheral nerves at either Day 27 (Fig. 1C) or Day 39 (Fig. 2C,O). Overall, PrP^C shared similar locations with nestin in bovine fetuses, including intermediate and marginal layers of the CNS, dorsal root ganglia and peripheral nerves. These regions are mainly populated by post-

mitotic neurons, which go through their last mitosis at the ventricular surface of the neuroepithelium and then migrate towards the opposite, marginal layers, where they differentiate [24].

PrP^C levels increase during ES cell differentiation

Expression of PrP^C during early development of the bovine nervous system in a developmentally- and spatially-regulated manner suggested that PrP^C might play a role in the nervous system development. However, experimental evaluation of this possibility is complicated in cattle due to their long gestation interval, expense and absence of convenient technologies (i.e. ES cells) to facilitate manipulation of gene expression. Thus, we chose to use differentiating murine ES cells as a model in which to test the role of PrP^C in the differentiation of neural cells.

ES cells differentiated into a variety of cell types during the 21-day culture period. A variety of cell morphologies were observed that corresponded to myoblast, fibroblast and neuroblast cell types (Fig. 3A). Spontaneously beating myoblasts appeared by Day 12 in all cultures. Western blot analysis revealed three PrP^C immunoreactive bands at 27, 32, and 35 kDa, presumably representing the non-, mono-, and di-glycosylated isoforms of PrP^C (Fig. 3B). The di-glycosylated isoform was most abundant, followed by the mono-glycosylated form. The non-glycosylated form was mainly detected after Day 12 of ES cell differentiation. Expression of the pluripotency marker Oct-4 declined significantly by Day 3 (0.63-fold relative to Day 0) and continued to decline through Day 21 (0.079-fold relative to Day 0; Fig. 3C). Conversely, expression of PrP^C protein, which is abundantly expressed in various differentiated cell types, increased significantly by Day 9 (3.7-fold relative to Day 0) and continued increasing through Day 18 (19-fold relative to Day 0; Fig. 3C). Similarly, Prnp mRNA expression increased significantly on Day 9 (1.8-fold relative to Day 0) and continued to rise through Day 18 (3.9-fold relative to Day 0; Fig. 3D). Collectively, these data indicated that Oct-4 expression was progressively reduced, whereas PrP^C levels were up-regulated during ES cell spontaneous differentiation.

Retinoic Acid promotes up-regulation of PrP^C during ES cell differentiation

Retinoic acid has been shown to promote neural differentiation in ES cells [25]. In this experiment, we evaluated whether RA would similarly promote differentiation of PrP^C-expressing cells. To address this question, ES cells were cultured in suspension under differentiating conditions to induce EB formation as in the preceding experiment. Retinoic acid was added from Day 4 to Day 8 as described in Materials and Methods. Contemporary control cultures were treated in an identical manner but without RA. Intense and progressive neuritogenesis was observed in RA-treated ES cells since Day 12 until Day 20 of differentiation compared to untreated controls (Fig. 4A). Oct-4 was monitored by quantitative Western blot as measure of ES cell differentiation (Fig. 4B). As in the previous experiment, Oct-4 levels declined rapidly in both treatments by Day 4 (Fig. 4C). On Day 8, Oct-4 levels were lower in RA-treated cultures compared to controls indicating that RA hastened the loss of pluripotent cells from the initial ES cell population. From Days 12 to 20, Oct-4 expression had stabilized to similarly low levels in both treatments. Nestin expression was measured to monitor the presence of neuroprogenitor cells during differentiation. Levels of nestin remained relatively low in both treatments until Day 12, when nestin expression rose sharply in the RA-treated cultures (26.5-fold relative to Day 0, vs. 1.4-fold in the untreated control; Fig. 4D). This difference persisted through Day 16, when higher levels of nestin were detected in the RA-treated ES cell compared to the untreated control (28.4-fold for RA vs. 11.8-fold for control). By Day 20, nestin expression in the controls rose to a level similar to that in the RA treatment. Thus, RA hastened the appearance of nestin-expressing cells during ES cell differentiation. PrP^C expression rose to

similar levels in both RA and control cultures from Day 4 to 16; however, by Day 20, PrP^C levels were significantly higher in the RA treatment (43-fold vs. 25-fold for the untreated control; Fig. 4C). Western blots were also probed for MAP-1 as a marker of post-mitotic neuron formation. However, we were unable to detect MAP-1 at any stage in either treatment (data not shown). The results of this experiment confirm the well-established effect of RA on promoting neural progenitor cell differentiation in ES cells [25]. The positive association displayed by PrP^C and nestin during ES cell differentiation corresponded with the pattern of expression observed across the neuroepithelium in bovine fetuses.

PrP^C contributes to ES cell differentiation into the neural lineage

PrP^C has been implicated in the proliferation and differentiation of neural progenitor cells [25]. We investigated whether PrP^C might play a role in the neural differentiation of ES cell. To test this possibility, a line of ES cells harboring a transgene designed to express a siRNA directed against PrP mRNA was established. Considering the positive association between nestin and PrP^C levels in the previous experiments, we hypothesized that reduction in PrP^C levels negatively affect nestin expression. ES cells were transfected with pSUPER.neo vector (Fig. 5B) containing a siRNA target sequence directed against the PrP^C mRNA coding region (Fig. 5A). siRNA-mediated knockdown of PrP^C resulted in lower ($P < 0.05$) PrP^C expression at Days 16 (70.9 %) and 20 (60%) compared to ES cells expressing the scrambled control sequence (Fig. 6A,B). Similarly, PrP^C mRNA levels in siRNA-PrP^C ES cells were decreased by 48.8 % and 53.1 % at Days 16 and 20, respectively compared to the scrambled control (Fig. 6C). Oct-4 expression decreased at Day 8 after RA induction in both groups; however, no differences were found between treatments (Control=0.036-fold and PrP^C siRNA=0.14-fold) (Fig. 6A,B). PrP^C siRNA cells showed less ($P < 0.05$) nestin expression at Day 16 (61.3 %) and Day 20 (70.7%) compared to the scrambled control (Fig. 6A,D). Corresponding with these results, immunofluorescence analyses showed co-localization of PrP^C and nestin and lower levels of both proteins in PrP^C siRNA cells compared to scrambled controls (Fig. 6E). These experiments indicate a spatial and temporal association between PrP^C and nestin during ES cell differentiation and provide evidence for the contribution of PrP^C in the differentiation of nestin-positive progenitor cells along the neural lineage.

DISCUSSION

In the present study we evaluated the spatial expression of PrP^C in the fetal bovine nervous system. Specifically, we investigated the extent to which PrP^C co-localized with nestin, a marker of neural stem cells [26] or MAP-2 a marker of mature post-mitotic neurons [27]. The expression and distribution of PrP^C, nestin and MAP-2 has not been described in fetal bovine nervous system. However, in fetal mice, proliferating neural stem and progenitor cells that express nestin are concentrated in the periventricular layer [28]. Maturing and post-mitotic neurons migrate away from the periventricular layer into the intermediate and marginal layers [29]. These cells then cease to express nestin and begin expressing MAP-2. In Day 27 and Day 39 bovine fetuses, we detected nestin expression mainly in the periventricular layer and to a lesser extent in the intermediate and marginal layers (Fig. 1F). The presence of nestin in these outer layers was unexpected; however, these regions contain radial glial cells in the developing fetal nervous system. Radial glial cells are transient, nestin-expressing cells that span the entire neuropithelium in the developing brain [30]. It is likely that the nestin-expressing cells detected in the intermediate and marginal layers are radial glial cells, though we did not confirm this in our study. MAP-2 was not detected in the periventricular layer, but as expected was expressed in the intermediate and marginal layers (Fig. 1G). PrP^C was localized mainly in the intermediate and marginal layers of the

neuroepithelium and was undetectable in periventricular layer (Fig. 1E). Thus, on Day 27 PrP^C appeared to be expressed in regions occupied by maturing and mature neurons and not in regions occupied by proliferating neural stem and progenitor cells.

The organization of proliferating stem cells, maturing and mature neurons was similar in the developing spinal cord. Nestin was clearly detected in the intermediate and marginal layers (Fig. 1J) and in dorsal root ganglia (Fig. 1N). MAP-2 expression in the spinal cord was strongest in the intermediate layer, weaker in the marginal layer (Fig. 1K) and quite strong in the dorsal root ganglia (Fig. 1O). PrP^C was detected in the intermediate and marginal layers of the spinal cord (Fig. 1I) and in the dorsal root ganglia (Fig. 1M). As in the brain, PrP^C in the spinal cord in Day 27 fetuses co-localized with regions that expressed both nestin and MAP-2.

The distribution of PrP^C in the neural tissues of Day 39 fetuses resembled that on Day 27; however, the tissue stained was more intense, suggesting higher levels of expression. In the brain, nestin was detected in throughout the neuroepithelium (Fig. 2F), while MAP-2 was confined to the intermediate layer (Fig. 2G). Interestingly, PrP^C staining was observed primarily in the marginal and outer intermediate layers (Fig. 2E). Expression of PrP^C and both markers followed a similar pattern in the spinal cord (Fig. 2, I–K). The marginal layer is rich in dendrites and axons and further in development will be part of the gray matter where most of PrP^C is localized at the adult stage [31,32]. The absence of MAP-2 from the marginal layer may be explained by the reduced role of MAP-2 after establishment of synaptic contact and stable cytoskeleton in differentiated neurons [33].

The distribution of PrP^C in the developing nervous system of cattle as shown here, as well as in mice [15] and humans [32] suggest that PrP^C plays a functional role in neural development. While PrP null mice display no overt neural phenotype [8], numerous subtle phenotypes have been reported (reviewed by [34]), including reduction in the number of neural precursor cells in developing mouse embryos [12]. Other studies have shown that PrP^C induced neuritogenesis in embryonic hippocampal neurons cultured in vitro [16,35]. In light of these observations, we sought to test the hypotheses that 1) PrP^C was expressed in differentiating ES cells and 2) Prnp knockdown would reduce the differentiation of murine ES cells into neural lineages. We found that when ES cells were cultured under differentiating conditions, PrP^C was expressed beginning on Day 9 after the onset of differentiation and increased through Day 21 (Fig. 3B–D). Retinoic acid has been shown to enhance differentiation of ES cells into neural lineages [19]. In our study, addition of retinoic acid to differentiating ES cells hastened the loss of pluripotency (as evidenced by more rapid decline in Oct-4 compared to controls; Fig. 4C) and differentiation into PrP^C- and nestin-expressing cells (Fig. 4B–D). However, we did not detect MAP-2 expression at any point during the 20-day culture period (data not shown) suggesting that the period analyzed in our experiments was insufficient to cover the emergence of more mature neurons capable of expressing MAP-2. Others have reported the differentiation of MAP-2 expressing cells from ES cells, albeit with different neural induction protocols than we used here [36] and after longer time periods [37].

Progressive neurite formation was observed in ES cell cultures starting on Day 12, when levels of PrP^C rose significantly (Fig. 4A,C). Previous studies have showed intense PrP^C expression in neurites [31] and our analysis detected strong PrP^C immunostaining in the marginal layer of the neuroepithelium where differentiated neurons extend dendrites and axons. This data suggests a close association between neuritogenesis and PrP^C expression. In our study, treatment of ES cells with RA for four days resulted in more intense neuritogenesis, greater levels of PrP^C and earlier loss of pluripotency evidenced by the decrease in Oct-4 levels at Day 8 (Fig. 4A–C). In order to analyze the fate of the ES cell

population, we measured nestin expression to estimate the proportion of cells following the neural stem/progenitor lineage. We found that RA induced an early up-regulation of nestin expression at Day 12 of differentiation compared to Day 16 of the untreated control. This pattern of expression, along with the greater expression of PrP^C and lower levels of Oct-4 suggests that RA induced earlier differentiation of ES cells along neural stem/precursor derivatives.

To test whether PrP^C played a role in the differentiation of nestin-expressing cells, we developed a clonal line of ES cells that expressed a PrP^C siRNA from a stably integrated transgene. PrP^C expression in differentiated derivatives of this cell line was knocked down by up to 75% (Day 16, Fig. 6B). Knockdown of PrP^C during differentiation did not affect the trajectory of decline in Oct-4 expression (Fig. 6B) suggesting that reduced levels of PrP^C expression had no general effect on loss of pluripotency. Interestingly, the onset of nestin expression was delayed in PrP knockdown cultures (Fig. 6C) suggesting that PrP^C influences the differentiation of nestin-expressing cell lineages, including neural lineages. This data was previously supported by the corresponding pattern of expression displayed by PrP^C and nestin across the neuroepithelium. These results are consistent with other reports arguing that PrP^C participates in cellular differentiation [38,12,39]. Moreover, our data in mouse ES cells agree with recent findings in human ES [40] supporting the hypothesis that PrP^C is involved in regulating ES cell differentiation status. The use of differentiating ES cells as a model for the study of PrP^C interactions with other cellular markers can provide more clues about the signaling pathways that mediate this function.

CONCLUSIONS

The expression of the mammalian PrP^C in the neuroepithelium and its spatial and temporal relation with neural markers nestin and MAP-2 suggest the participation of PrP^C in the process of neural differentiation during early embryogenesis. The use of ES cells to study the potential role or PrP^C in neurogenesis allowed us to show how PrP^C is up-regulated during differentiation of stem/progenitor cells. Moreover, in the present work we provided evidence for the positive association between PrP^C and nestin expression indicating the contribution of PrP^C in neurogenesis.

ABBREVIATIONS

PrP^C	cellular prion protein
PrP^{Sc}	scrapie prion protein
Prnp	prion gene
TSE	transmissible spongiform encephalopathy

Acknowledgments

LITARATURE CITED

1. McKinley MP, Taraboulos A, Kenaga L, Serban D, Stieber A, DeArmond SJ, Prusiner SB, Gonatas N. Ultrastructural localization of scrapie prion proteins in cytoplasmic vesicles of infected cultured cells. Lab. Invest 1991;65:622–630. [PubMed: 1684401]

2. Taraboulos A, Jendroska K, Serban D, Yang SL, DeArmond SJ, Prusiner SB. Regional mapping of prion proteins in brain. Proc. Natl. Acad. Sci. USA 1992;15:7620–7624. [PubMed: 1354357]

3. Caughey BW, Dong A, Bhat KS, Ernst D, Hayes SF, Caughey WS. Secondary structure analysis of the scrapie-associated protein PrP 27–30 in water by infrared spectroscopy. Biochemistry 1991;30:7672–7680. [PubMed: 1678278]

4. Pan KM, Baldwin M, Nguyen J, Gasset M, Serban A, Groth D, Mehlhorn I, Huang Z, Fletterick RJ, Cohen FE, Prusiner SB. Conversion of alpha-helices into beta-sheets features in the formation of the scrapie prion proteins. Proc. Natl. Acad. Sci. USA 1993;90:10962–10966. [PubMed: 7902575]

5. Vasallo N, Herms J. Cellular prion protein function in copper homeostasis and redox signaling at the synapse. J. Neurochem 2003;86:538–544. [PubMed: 12859667]

6. Bounhar Y, Zhang Y, Goodyer CG, LeBlanc A. Prion protein protects human neurons against Bax-mediated apoptosis. J. Biol. Chem 2001;276:39145–39149. [PubMed: 11522774]

7. Roucou X, Giannopoulos PN, Zhang Y, Jodoin J, Goodyer CG, LeBlanc A. Cellular prion protein inhibits proapoptotic Bax conformational change in human neurons and in breast carcinoma MCF-7 cells. Cell. Death. Differ 2005;12:783–795. [PubMed: 15846375]

8. Bueler H, Fischer M, Lang Y, Fluethmann H, Lipp HP, DeArmond SJ, Prusiner SB, Aguet M, Wissmann C. Normal development and behavior of mice lacking the neuronal cell-surface PrP protein. Nature 1992;356:577–582. [PubMed: 1373228]

9. Bueler H, Aguzzi A, Sailer A, Greiner RA, Autenried P, Aguet M, Weissmann C. Mice devoid of PrP are resistant to scrapie. Cell 1993;73:1339–13347. [PubMed: 8100741]

10. Mouillet-Richard S, Ermonval M, Chebassier C, Laplanche JL, Lehmann S, Launay JM, Kellermann O. Signal transduction through prion protein. Science 2000;289:1925–1928. [PubMed: 10988071]

11. Zhang CC, Steele AD, Lindquist SL, Lodish HF. Prion protein is expressed on long-term repopulating hematopoietic stem cells and is important for their self-renewal. Proc. Natl. Acad. Sci. USA 2006;103:2184–2189. [PubMed: 16467153]

12. Steele AD, Emsley JG, Ozdinler PH, Lindquist S, Macklis J. Prion protein (PrPC) positively regulates neural precursor proliferation during developmental and adult mammalian neurogenesis. Proc. Natl. Acad. Sci. USA 2006;103:3416–3421. [PubMed: 16492732]

13. Manson J, West JD, Thomson V, McBride P, Kaufman MH, Hope J. The prion protein gene: a role in mouse embryogenesis? Development 1992;115:117–122. [PubMed: 1353438]

14. Miele G, Alejo Blanco AR, Baybutt H, Horvat S, Manson J, Clinton M. Embryonic activation and developmental expression of the murine prion protein gene. Gene Expression 2003;11:1–12. [PubMed: 12691521]

15. Tremblay P, Bouzamondo-Bernstein E, Heinrich C, Prusiner SB, DeArmond SJ. Developmental expression of PrP in the post-implantation embryo. Brain. Res 2007;30:60–67. [PubMed: 17292334]

16. Kanaani J, Prusiner SB, Diacovo J, Baekkeskov S, Legname G. Recombinant prion protein induces rapid polarization and development of synapses in embryonic rat hippocampal neurons in vitro. J. Neurochem 2005;95:1373–1386. [PubMed: 16313516]

17. Winters, LM.; Green, WW.; Comstock, RE. Prenatal development of the bovine. Technical Bulletin, Minnesota Agricultural Experiment Station; 1942.

18. Rudnicki, M.; McBurney, MW. Cell culture methods and induction of differentiation of embryonal carcinoma cell lines. In: Robertson, EJ., editor. Teratocarcinomas and embryonic stem cells a practical approach. Washington, DC: IRL Press; 1987. p. 19-49.

19. Bain G, Kitchens D, Yao M, Huettner JE, Gottlieb DI. Embryonic stem cells express neuronal properties in Vitro. Dev. Biol 1995;168:342–357. [PubMed: 7729574]

20. Brummelkamp TR, Bernards R, Agami R. A system for stable expression of short interfering RNAs in mammalian cells. Science 2002;296:550–553. [PubMed: 11910072]

21. Fishell G, Mason CA, Hatten ME. Dispersion of neural progenitors within the germinal zones of the forebrain. Nature 1993;362:636–638. [PubMed: 8464514]

22. Komatsu F, Farkas I, Akatsu H, Kojima K, Fukushima T, Okada H. Potential neural progenitor cells in fetal liver and regenerating liver. Cytotechnology 2008;56:209–217. [PubMed: 19002859]

23. Kachinsky AM, Dominov JA, Miller JB. Intermediate filaments in cardiac myogenesis: Nestin in the developing mouse heart. J. Histochem. Cytochem 1995;43:843–847. [PubMed: 7542682]

24. Frederiksen K, McKay RDG. Proliferation and differentiation of rat neuroepithelial precursor cells in vivo. J. Neurosci 1988;8:1144–1151. [PubMed: 3357014]

25. Kim M, Habiba A, Doherty JM, Mills JC, Mercer RW, Huettner JE. Regulation of mouse embryonic stem cell neural differentiation by retinoic acid. Dev. Biol 2009;15:456–471. [PubMed: 19217899]

26. Lendahl U, Zimmerman LB, McKay RD. CNS stem cells express a new class of intermediate filament protein. Cell 1990;23:585–595. [PubMed: 1689217]

27. Johnson GV, Jope RS. The role of microtubule-associated protein 2 (MAP-2) in neuronal growth, plasticity, and degeneration. J. Neurosci. Res 1992;33:505–512. [PubMed: 1484385]

28. Kawaguchi A, Miyata T, Sawamoto K, Takashita N, Murayama A, Akamatsu W, Ogawa M, Okabe M, Tano Y, Goldman SA, Okano H. Nestin-EGFP transgenic mice: visualization of the self-renewal and multipotency of CNS stem cells. Mol. Cell. Neurosci 2001;17:259–273. [PubMed: 11178865]

29. Temple S. The development of neural stem cells. Nature 2001;414:112–117. [PubMed: 11689956]

30. Kriegstein AR, Gotz M. Radial glia diversity: a matter of cell fate. Glia 2003;43:37–43. [PubMed: 12761864]

31. Sales N, Hassig R, Katia R, Giamberardino LD, Traiffort E, Ruat M, Fretier P, Moya L. Developmental expression of the cellular prion protein in elongating axons. Eur. J. Neurosci 2002;15:1163–1177. [PubMed: 11982627]

32. Adle-Biassette H, Verney C, Peoc'h K, Dauge MC, Razavi F, Choudat L, Gressens P, Budka H, Henin D. Immunohistochemical expression of prion protein (PrPC) in the human forebrain during development. J. Neuropathol. Exp. Neurol 2006;65:698–706. [PubMed: 16825956]

33. Sanchez C, Diaz-Nido J, Avila J. Phosphorylation of microtubule-associated protein 2 (MAP2) and its relevance for the regulation of the neuronal cytoskeleton function. Prog. Neurobiol 2000;61:133–168. [PubMed: 10704996]

34. Steele AD, Lindquist S, Aguzzi A. The Prion Protein Knockout Mouse: A Phenotype Under Challenge. Prion 2007;1:83–93. [PubMed: 19164918]

35. Lopes MH, Hajj GN, Muras AG, Mancini GL, Castro RM, Ribeiro KC, Brentani RR, Linden R, Martins VR. Interaction of cellular prion and stress-inducible protein 1 promotes neuritogenesis and neuroprotection by distinct signaling pathways. J. Neurosci 2005;25:11330–11339. [PubMed: 16339028]

36. Nishimura F, Toriumi H, Ishizaka S, Sakaki T, Yoshikawa M. Use of differentiating embryonic stem cells in the Parkinsonian mouse model. Methods Mol. Biol 2006;329:485–493. [PubMed: 16846012]

37. Lee DH, Koo DB, Ko K, Ko K, Kim SM, Jung JU, Ryu JS, Jin JW, Yang HJ, Do SI, Jung KY, Choo YK. Effects of daunorubicin on ganglioside expression and neuronal differentiation of mouse embryonic stem cells. Biochem. Biophys. Res. Commun 2007;362:313–318. [PubMed: 17707770]

38. Dodelet VC, Cashman NR. Prion protein expression in human leukocyte differentiation. Blood 1998;91:1556–1561. [PubMed: 9473220]

39. Pantera B, Bini C, Cirri P, Paoli P, Camici G, Manao G, Caselli A. PrPc activation induces neurite outgrowth and differentiation in PC12 cells: role for caveolin-1 in the signal transduction pathway. J. Neurochem 2009;110:194–207. [PubMed: 19457127]

40. Lee YJ, Baskakov IV. Treatment with normal prion protein delays differentiation and helps to maintain high proliferation activity in human embryonic stem cells. J. Neurochem 2010;114:362–373. [PubMed: 20089130]
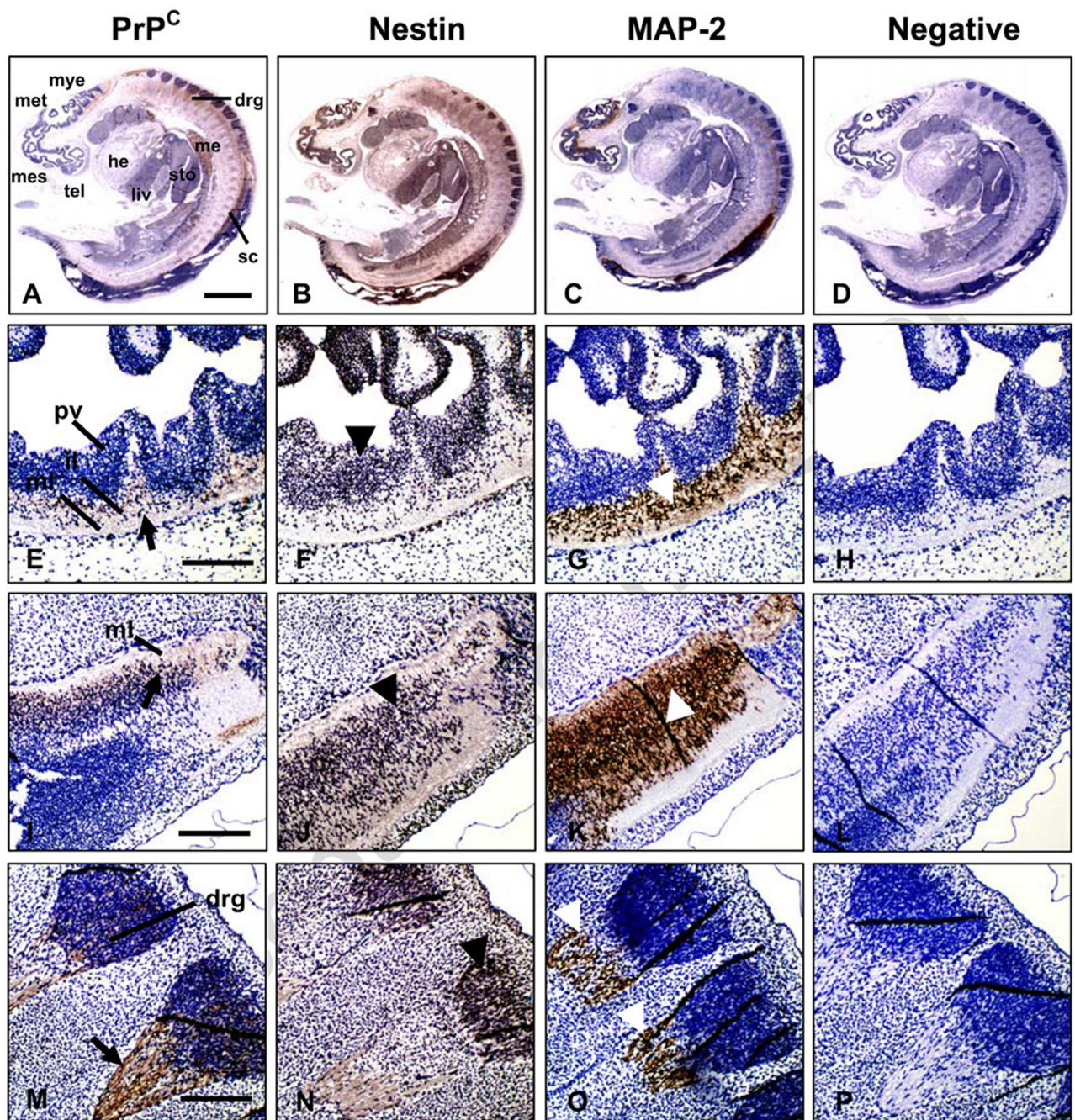
Figure 1.
Immunohistochemical analysis of PrP^C, nestin and MAP-2 expression in Day-27 bovine fetuses. Sagittal sections of whole fetuses show immunoreactivity for (A) PrP^C, (B) nestin and (C) MAP-2 mainly associated to the CNS and peripheral nerves. Specific PrP^C staining (black arrow) was detected in the intermediate (il) and marginal (ml) layers of the developing (E) brain, (I) spinal cord and (M) dorsal root ganglia (drg). Nestin (black arrow-head) showed a wide pattern of staining mainly localized in the periventricular (pv) layer of the (F) brain, (J) spinal cord and (N) dorsal root ganglia. MAP-2 expression (white arrow-head) was observed in the marginal and intermediate layers of (G) developing brain, (K) spinal cord and (O) dorsal root ganglia. (D, H, L and P) Negative control incubated with

non-immune horse serum instead of primary antibody. Abbreviations: he; heart; mes, mesencephalon; met, metencephalon; mye, myelencephalon, me, mesonephros; liv, liver; sc, spinal cord; sto, stomach. Bar scale: (A–D) 500 µm; (E–P) 100 µm.
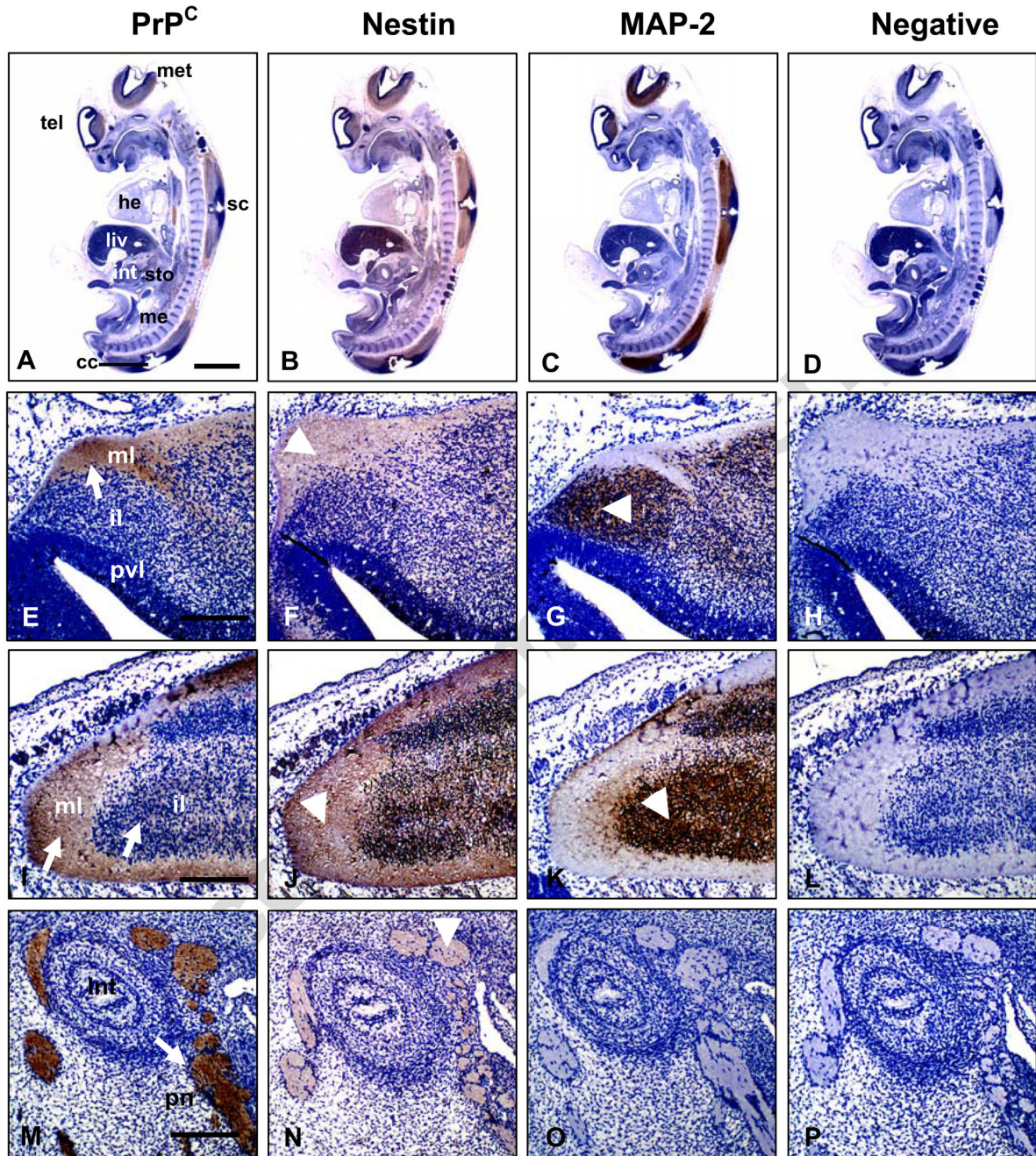
Figure 2.
Immunohistochemical analysis of PrP^C, nestin and MAP-2 expression in Day-39 bovine fetuses. Sagittal sections of whole fetuses show immunoreactivity for (A) PrP^C, (B) nestin and (C) MAP-2 mainly associated to the CNS and peripheral nerves. Specific PrP^C staining (white arrow) was detected in the intermediate (il) and marginal (ml) layers of (E) developing brain, (I) spinal cord and (M) peripheral nerves (pn) associated to the intestine. Nestin (white arrow-head) showed a wide pattern of staining mainly localized in the marginal and intermediate layers of the (F) brain, (J) spinal cord and (N)peripheral nerves. MAP-2 expression (white arrow-head) was observed in intermediate layer of the (G) brain, (K) spinal cord; however no staining was detected in (O) peripheral nerves. (D, H, L and P)

Negative control incubated with non-immune horse serum instead of primary antibody. Abbreviations: he, heart; met, metencephalon; me, mesonephros; liv, liver; sc, spinal cord; sto, stomach; tel, telencephalon. Bar scale: (A–D) 500 µm; (E–P) 100 µm.

A

Undifferentiated   Myoblast

Fibroblast   Neuroblast

B

C

D
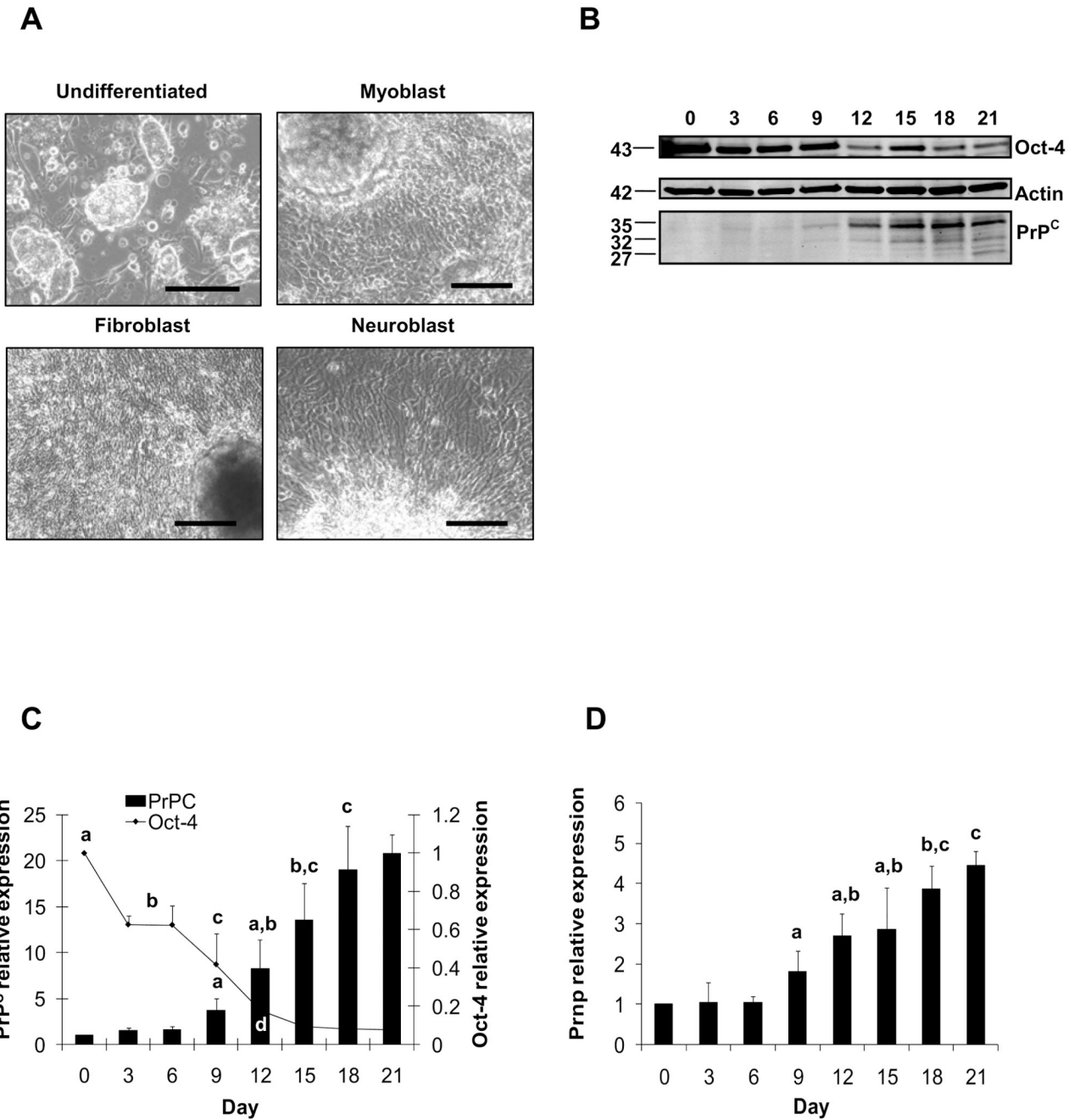
Figure 3.
Expression of PrP^C and Oct-4 in differentiating mouse ES cells. (A) ES cells were differentiated after 21 days in culture into predominant neuroblast, myoblast and fibroblast cells. (B) PrP^C displayed immunoreactive bands at 35, 32 and 27 kDa with Oct-4 reactivity at 43 kDa and control β-actin at 42 kDa. Computerized quantification of migration bands showed that PrP^C expression was significantly (P < 0.05) higher since Day 9 of differentiation. (C) Oct-4 expression showed lower (P < 0.05) values since Day 3 of differentiation. (D) PrP^C mRNA values were significantly (P < 0.05) greater after Day 9 of differentiation. For PrP^C and Oct-4 levels, superscripts (a,b,c,d) represent significant (P <

0.05) differences between sampling days. Bar scale pictures: (Up-left) 500 µm; (Up-right) 200 µm; (Down-left) 200 µm; (Down-right) 200 µm.
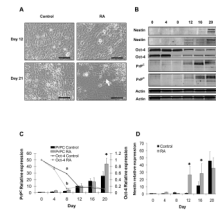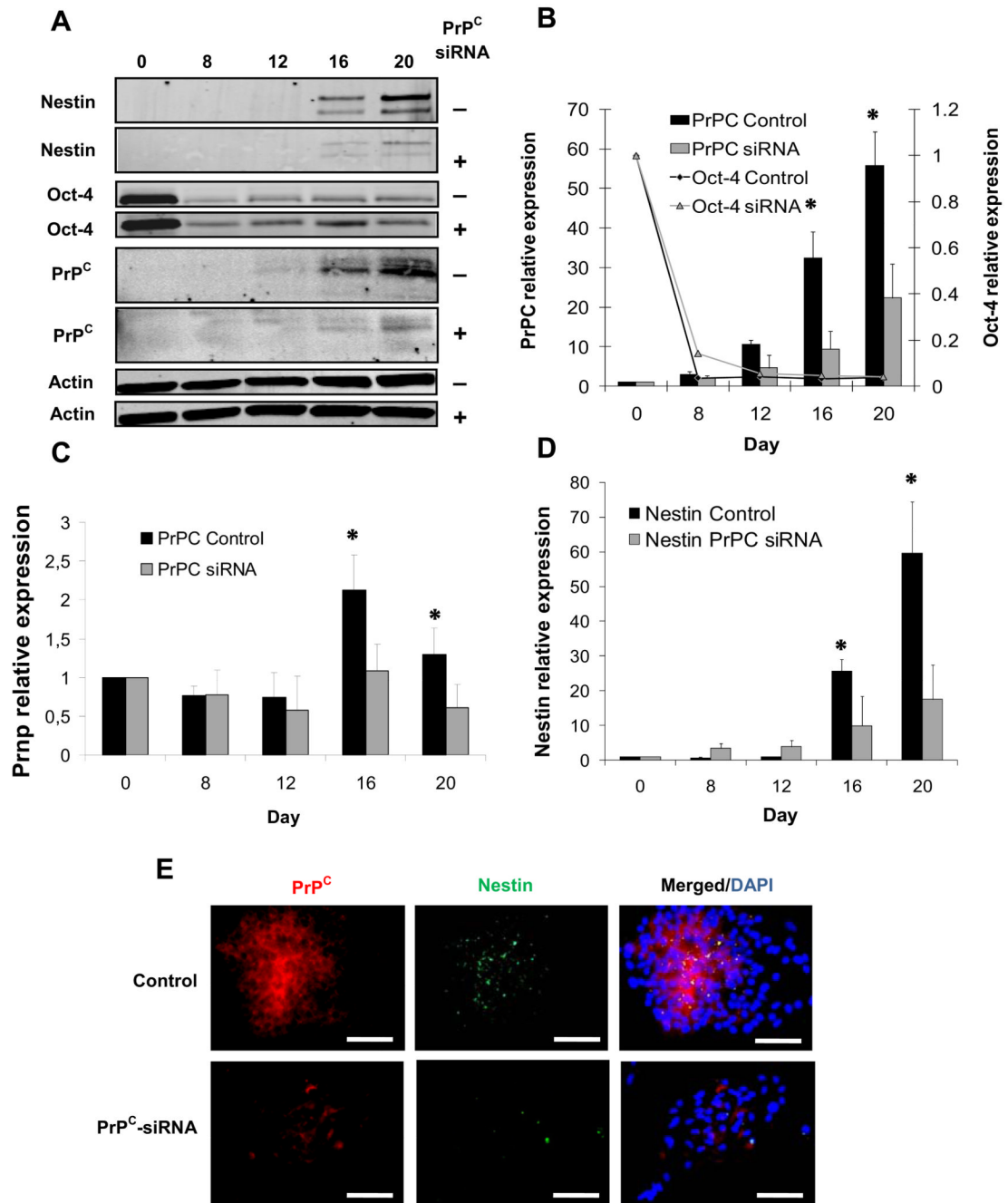
Figure 4.
Expression of PrP^C, Oct-4 and nestin in differentiating ES cell after induction with RA. (A) RA-treated ES cells showed intense neuritogenesis since Day 12 through Day 20 (white arrow). (B) PrP^C displayed immunoreactive bands at 35, 32 and 27 kDa. Reactivity was also detected for Oct-4, β-actin and nestin at 43, 42, 120 kDa, respectively. (C) Computerized quantification of migration bands showed a higher ($P < 0.05$) expression of PrP^C in RA-treated ES cells compared to the controls at Day 20 of differentiation. Oct-4 showed lower ($P < 0.05$) levels in RA-treated ES cells since Day 8 compared to untreated control. (D) RA-treated ES cells displayed greater ($P < 0.05$) levels of nestin at Days 12 and 16 compared to controls. For PrP^C and Oct-4 levels, superscripts (a,b,*) represent significant ($P < 0.05$) differences between sampling days. Bar scale pictures: (Left) 100 µm; (Right) 200 µm.
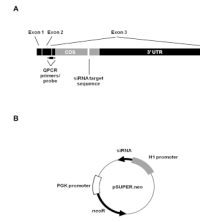
Figure 5.
Structure of the PrP^C mRNA and pSUPER.neo vector used to target PrP^C mRNA expression. (A) Bovine PrP^C mRNA showing location of siRNA target sequence, probe and primer location for QPCR. pSUPER.neo vectordriven by the H1 RNA promoter, yields mRNA that contains two 19-base pallindromic targeting sequences separated by nine bases that form a hairpin loop after folding of the pallindromes to form a double-stranded RNA. (B) Control vector was identical, save for substitution of a scrambled version of the targeting sequence.

Figure 6.
Expression of PrP^C, Oct-4 and nestin in differentiating ES cells after siRNA-mediated knockdown of PrP^C. (A) PrP^C displayed immunoreactive bands at 35, 32 and 27 kDa. Reactivity was also detected for Oct-4, β-actin and nestin at 43, 42, 120 kDa, respectively. (B) Computerized quantification of migration bands indicated that PrP^C expression was significantly reduced (P < 0.05) on Days 16 and 20 compared to scrambled control. Oct-4 levels were reduced at Day 8 with no differences between treatments. (C) PrP^C mRNA levels were reduced in siRNA-PrP^C ES cells at Days 16 and 20 compared to controls. (D) siRNA-PrP^C ES cells showed lower levels of nestin levels on Days 16 and 20 compared to scrambled control. (E) PrP^C and nestin immunoreactive signals were reduced in siRNA-

PrP^C ES cells compared to control colonies at day 20 of differentiation. Merged PrP^C, nestin and DAPI for (e) scrambled control and (f) siRNA ES cells. Superscript (*) indicate significant (P < 0.05) difference. Bar scale pictures: (Up-left) 500 µm; (Up-right) 200 µm; (Down-left) 200 µm; (Down-right) 200 µm. Bar scale pictures: 200 µm.